Numerical Simulation of the Flow Behavior and Breakthrough Phenomenon in Co-Injection Molding

Ilinca, Florin; Hétu, Jean-François

Publisher's version / Version de l'éditeur:

Proceedings of the 9th International Conference on Numerical Methods in Industrial Forming Processes, 2007., 2007-06-21

Numerical Simulation of the Flow Behavior and Breakthrough Phenomenon in Co-Injection Molding

Florin Ilinca and Jean-François Hétu

National Research Council, Industrial Materials Institute
75 de Mortagne, Boucherville, Québec, Canada, J4B 6Y4

Abstract. A study of the flow behavior during sequential co-injection molding is shown using a three-dimensional finite element flow analysis code. Solutions of the non-Newtonian, non-isothermal melt flow are obtained by solving the momentum, continuity and energy equations. Two additional transport equations are solved for tracking polymer/air and skin/core polymers interfaces. The co-injection model is integrated into the NRC's 3D injection molding software. Solutions are shown for the filling of a spiral-flow mould for which experimental measurements are available. The numerical approach predicts the core advance stage during which the core flow front catches up on the skin flow front and the core expansion phase when the flow fronts of core and skin materials advance together without breakthrough. The breakthrough phenomenon is also predicted. The predicted flow front behavior is compared to the experimental observations for various skin/core melt temperature and skin/core viscosity ratio. Simulation results are in good agreement with experimental data and indicate correctly the trends in solution change when processing parameters are changing.

Keywords: Co-Injection, 3D Modeling, Finite Elements, Core shape, Core Breakthrough.

INTRODUCTION

Co-injection molding involves injection of skin and core polymer melt into a mold cavity such as the core material is embedded within the solidified layers of the skin material. Co-injection molding offer significant cost and quality advantages. The process has the potential of providing optimal properties of the molded part by using a proper combination of the skin and core materials. An elastomer skin over a rigid core will provide a solid structure with a soft touch. Meanwhile, a brittle material can be covered by one with high impact resistance or high ductility. Co-injection offers also the opportunity to reduce the production cost by using lower cost materials wherever a high performance material is not necessary, perhaps in the core. Co-injection is a very effective manufacturing technique for ensuring both high recycled material content and high quality product.

Getting the proper combination of two polymer resins into the same cavity makes co-injection molding more difficult than traditional injection. Very often the success in co-injection design comes at the end of a long trial and error learning process. Accurate numerical predictions of the process behavior can help the processors get the optimal design and can produce substantial investment savings in both time and money.

First attempts on the numerical simulation of co-injection molding were mostly based on the thin wall, Hele-Shaw approximation [1,2]. While for parts presenting thick sections such approach is clearly inappropriate, it shows that even for thin parts, a 2.5D approach may be rough, as the core polymer penetration is a three-dimensional phenomenon. In many applications, it is important to provide not only the depth of the core polymer penetration, but also details on the core shape and polymer skin thickness. Numerical prediction of core breakthrough is an even bigger challenge. Therefore, a true three-dimensional solution of the injection process is needed.

In previous work the authors elaborated a three-dimensional method for the simulation of co-injection molding [3-7]. The numerical approach provides the evolution of the polymer/air and core/skin interfaces and the final shape and depth of the core. The resolution of the true 3D mold-filling problem allows the computation of accurate and detailed information regarding the shape and the size of the core material, as well as the thickness of the skin. Those results are especially useful in critical regions such as near corners, obstacles, or in regions presenting changes in

CP908, *NUMIFORM '07, Materials Processing and Design: Modeling, Simulation and Applications*
edited by J. M. A. César de Sá and A. D. Santos
2007 American Institute of Physics 978-0-7354-0415-1/07/$23.00

part thickness. A robust and accurate solution algorithm will also provide the framework for detailed analysis of the role played by different parameters determining the final characteristics of the part. In such a way the prediction of an optimal design of the process using simulation is a realizable task.

This work details the numerical prediction of hard to simulate flow phenomena such as the core expansion phase during which the flow fronts of core and skin materials advance together without breakthrough. Solutions are shown for a spiral-flow mold for which experimental measurements are available. The breakthrough phenomenon is also predicted and the numerical solution is in good agreement with the experiment.

FINITE ELEMENT SOLUTION

The equations governing the incompressible melt flow are the Stokes equations and the continuity equation

$$0 = -\nabla p + \nabla \cdot (2\eta\dot{\gamma}(\mathbf{u})), \qquad (1)$$

$$-\nabla \cdot \mathbf{u} = 0, \qquad (2)$$

where $\dot{\gamma}(\mathbf{u}) = (\nabla\mathbf{u} + (\nabla\mathbf{u})^T)/2$ is the strain rate tensor.

Heat transfer is modeled by the energy equation:

$$\rho c_p \left(\frac{\partial T}{\partial t} + \mathbf{u} \cdot \nabla T \right) = \nabla \cdot (k \nabla T) + 2\eta\dot{\gamma}(\mathbf{u}). \qquad (3)$$

In the above equations, t, $\mathbf{u}$, p, T, ρ, η, c_p and k denote time, velocity, pressure, temperature, density, viscosity, specific heat and thermal conductivity respectively.

The position of the polymer/air and skin/core polymer interfaces is modeled using a pseudo-concentration method [8]. Smooth functions $F_i(x,t)$ such that the critical value, F_c, represents the position of the interface. The pseudo-concentration functions are transported using the velocity field provided by the solution of the momentum-continuity equations:

$$\frac{\partial F_i}{\partial t} + u \cdot \nabla F_i = 0 \qquad \text{on} \quad \Omega \qquad (4)$$

We consider i=1 and i=2 for the polymer/air and skin/core interfaces, respectively. A front tracking value greater than F_c denotes a region filled by the polymer. As two interfaces are present the various combinations are summarized in Table 1.

TABLE 1. Definition of filled (skin/core) and empty regions.

	$F_1 \geq F_c$	$F_1 < F_c$
$F_2 \geq F_c$	Core Polymer	Core breakthrough skin material
$F_2 < F_c$	Skin Polymer	Empty (air)

For velocity no-slip boundary conditions are imposed on the cavity walls filled by the polymer, while on the unfilled part, a free boundary condition allows for the formation of the typical fountain flow. The heat transfer between the cavity and the mold is given by

$$q_m = h_c (T - T_m) \qquad \text{on} \quad \Gamma_{\text{mold}}, \qquad (5)$$

where h_c is a surface heat transfer coefficient and T_m is the mold temperature.

Model equations are discretized in time using a first order implicit Euler scheme. Linear continuous interpolation functions are used for all variables. At each time step, the global system of equations is solved in a partly segregated manner: momentum-continuity ($\mathbf{u}$,p), energy (T), and then the front tracking equations (F_1,F_2). When the skin polymer is injected, only the front tracking function for polymer/air interface is solved, while during the core polymer injection both front tracking functions are computed [5].

NUMERICAL RESULTS

This application was the object of an experimental study by Watanabe et al. [9,10]. The mold has a spiral-flow cavity with 20mm width and 2mm thickness (see Figure 1).

For the reference simulation case, the molding material for both skin and core is PC (Panlite L-1225L). Material properties for the numerical simulation were:

- density, ρ=1200kg/m3,
- specific heat, c_p = 2000J/(kg ·ºC),
- thermal conductivity, k = 0.25W/(m·ºC).

The viscosity is modeled by the Cross-WLF model equations

$$\eta = \frac{\eta_0}{1 + \left(\eta_0 \dot{\gamma} / \tau^*\right)^{1-n}} \qquad (6)$$

$$\eta_0 = D_1 \exp\left\{ \frac{-A_1 (T - T^*)}{A_2 + (T - T^*)} \right\} \qquad (7)$$

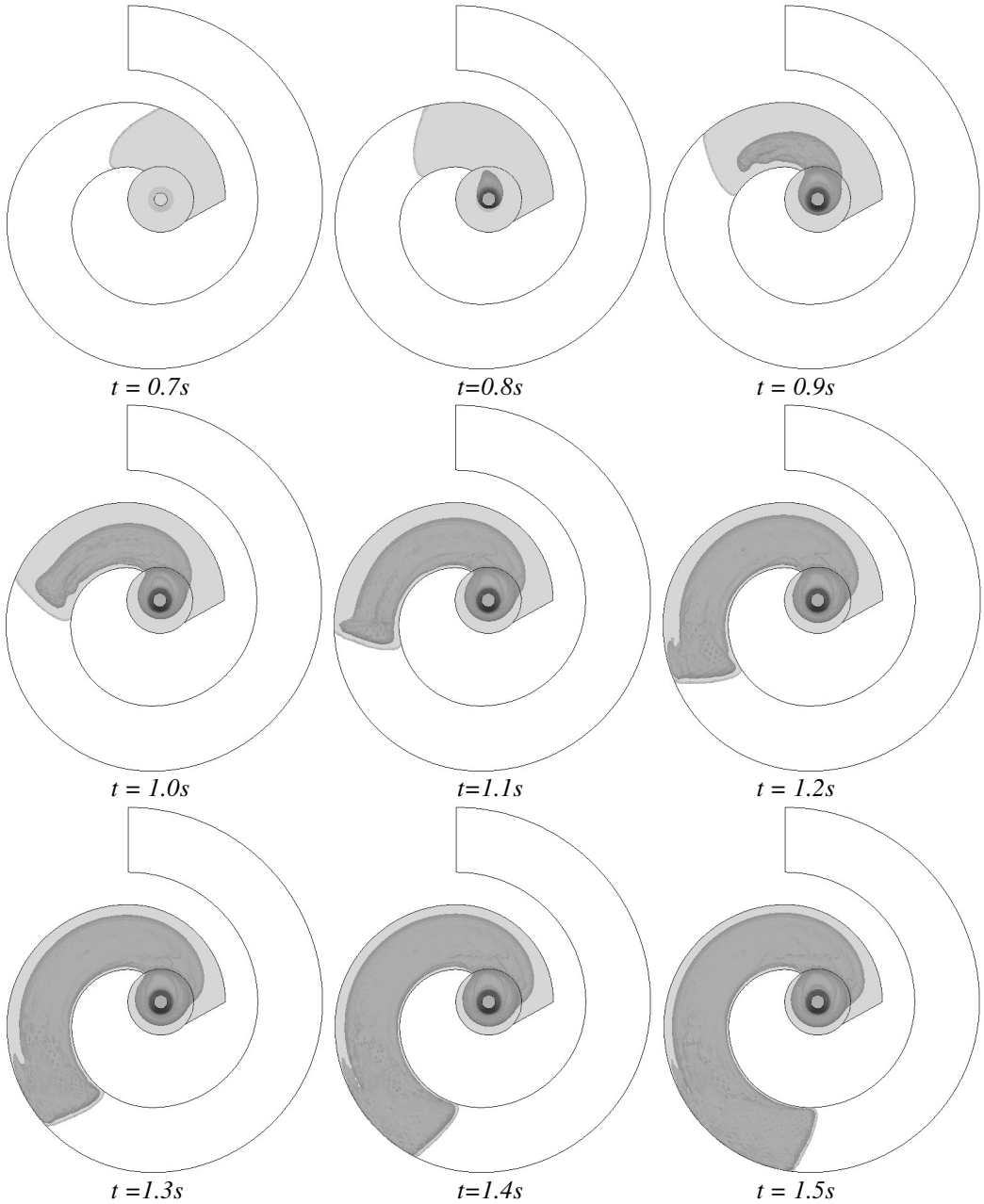

FIGURE 1. Spiral mold: evolution of the core penetration.

where $T^* = D_2 + D_3 p$, and $A_2 = \tilde{A}_2 + D_3 p$. Model constants used for the numerical simulation are summarized in Table 2.

TABLE 2. Cross-WLF model constants for Panlite L-1225L.

Model constant	Value
n ; τ^* (Pa)	0.12; $8.5 \cdot 10^5$
D_1 (Pa· s); D_2 (^{0}C); D_3 (^{0}C/Pa)	$2.5 \cdot 10^9$; 175.0; 0.0
A_1; $\tilde{A}_2$ (^{0}C)	22.0; 44.0

The melt is injected at 300ºC and the mold is kept at 80ºC. The core and skin materials were injected sequentially. The core material is injected at 0.7s when the flow length of skin material is about 30mm.

The position of skin and core materials at various times during the filling is shown in Figure 1. The skin material is plotted in light grey and the darker region indicates the core.

As can be seen the core material advances more rapidly than the skin. As a result the core catches up

on free surface of the skin material. The numerical solution for the skin and core flow lengths is compared with the experimental data of Watanabe et al. [9] in Figure 2. The numerical solution recovers the four experimentally observed regions of flow behavior:

(I) Primary injection phase: only skin material is injected and skin flow front progresses inside the cavity.

(II) Core advance region: the core material is injected and advances more rapidly than the skin, catching up on free surface of the skin.

(III) Core expansion region: once the flow front of core material catches up on the one of the skin material, the two flow fronts advance together without breakthrough.

(IV) Core breakthrough region: only the core material is found on the free surface. On the numerical simulation breakthrough is identified by the presence of the core material on the surface of the part.

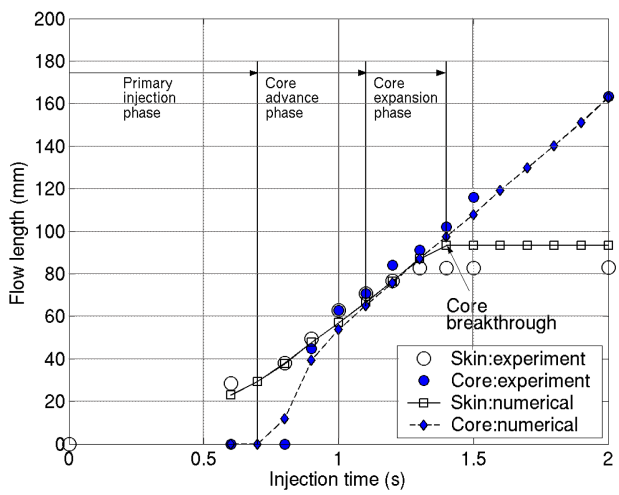

FIGURE 2. Skin and core position for spiral mold.

The numerical model results in accurate predictions and indicates correctly the core expansion phase between t = 1.1s and t = 1.4s. The material behavior during this period is very hard to predict numerically since the flow front of core and skin materials advance together without breakthrough. During the core advance phase the core flow front advances much faster than the skin material, whereas during the core expansion the core and skin fronts move together at almost the same speed. The layer of skin material at the interface with the mold and at the flow front is very thin and it is progressively stretched up to breakthrough. Breakthrough occurs at about t=1.4s close to the experimental observation. The numerical solution at the beginning of the core expansion phase and just prior to breakthrough is shown in Figure 3.

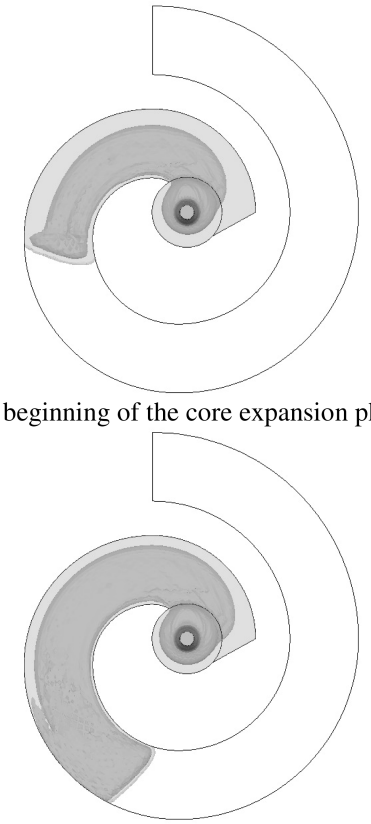

(a) beginning of the core expansion phase

(b) core breakthrough

FIGURE 3. Core penetration: (a) beginning of the core expansion phase (t=1.1s), (b) breakthrough (end of the core expansion phase, t=1.4s).

The flow behaviour of the skin and core materials was analyzed for various temperatures and viscosities of the skin material [11,12]. A summary of the simulations is shown in Table 3 (the reference case is identified as S-L). Computations were carried out for the cases for which materials with higher viscosity were used for the skin (S-M in Table 3 for skin polymer grade L-1250 with middle viscosity and S-H for skin polymer grade K-1300 with high viscosity). The case of skin material with higher viscosity was simulated for skin temperatures of 300ºC, 310ºC and 320ºC respectively (C-300, C-310 and C-320 in Table 3). Cases C-300 and S-H are the same.

TABLE 3. Summary of the molding conditions.

Case	Skin temp. (C)	Skin visc.	Core temp. (C)	Core visc.
C-300	300	High	300	Low
C-310	310	High	300	Low
C-320	320	High	300	Low
S-L	300	Low	300	Low
S-M	300	Middle	300	Low
S-H	300	High	300	Low

Solutions for various temperatures of the skin material are compared with the experimental data in Figure 4. The predicted moment when core material reaches the front of skin material (beginning of the core expansion phase) agrees very well with the experimental data for all three values of the skin temperature.

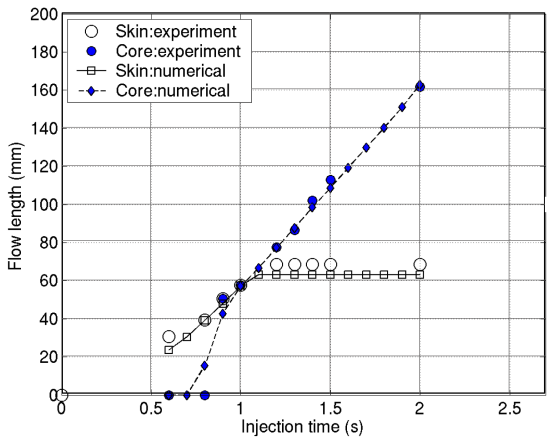

(a) Skin temperature = 300ºC

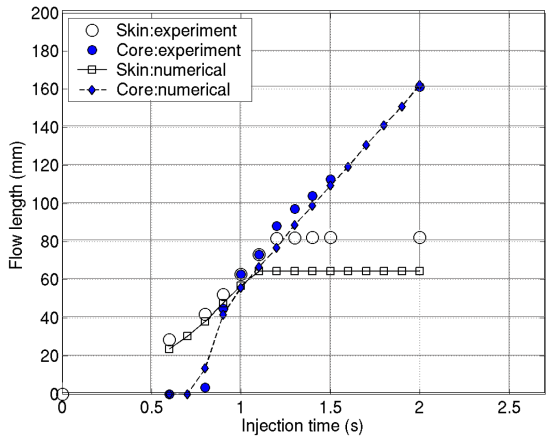

(b) Skin temperature = 310ºC

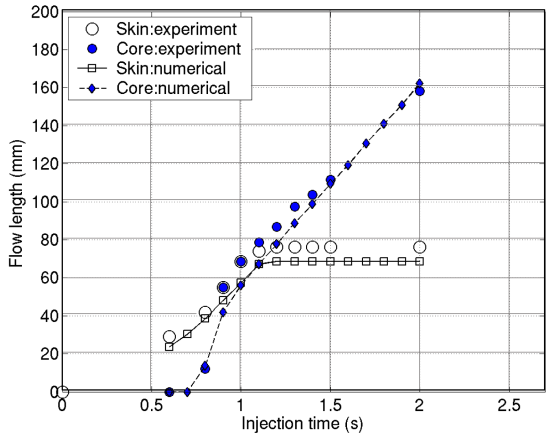

(c) Skin temperature = 310ºC

FIGURE 4. Flow length of skin/core material for various temperatures of skin material.

Numerical results underestimate the length of the core expansion region especially for the case of skin material injected at 310ºC as seen in Figure 5. However, the numerical model correctly indicates an increase in the length of the core expansion region as the temperature of the skin material increases.

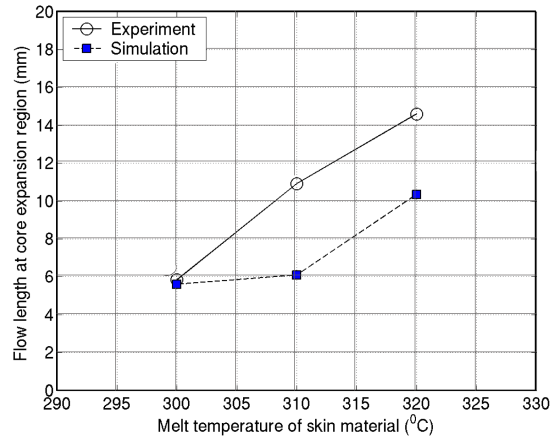

FIGURE 5. Flow length at core expansion region as function of the melt temperature of skin material.

The solutions obtained for various skin viscosities are compared with the experiment in Figure 6. In this case the agreement with the experimental observations is much improved. The length of the core expansion region agrees well with the measured values as shown in Figure 7. For skin materials having higher viscosities the breakthrough occurs sooner and the core expansion region is shorter. These results are in good agreement with the observations of Watanabe *et al.* [10].

CONCLUSION

This work presents a three-dimensional finite element method for solving the co-injection molding process. The procedure provides the evolution of the polymer/air and skin/core polymer interfaces and the final shape and depth of the core polymer. Solutions were presented for a spiral mold for which experimental data is available.

The proposed procedure is able to predict the core expansion phase, the core advance phase and the core breakthrough. It deals with changes in part thickness or flow direction, and provides all the needed information concerning skin thickness and core shape. It works in the same manner for thin parts and for thick three-dimensional parts.

Solutions for the spiral mold indicate a very good agreement between the numerical results and the experimental observations. Notably the simulation

predicts correctly the beginning of the core expansion phase (the moment when the core material catches up on the front of skin material) and the occurrence of core breaking through the skin.

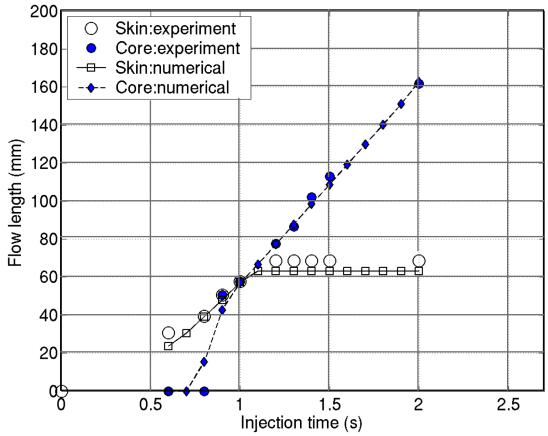

(a) Skin viscosity = high

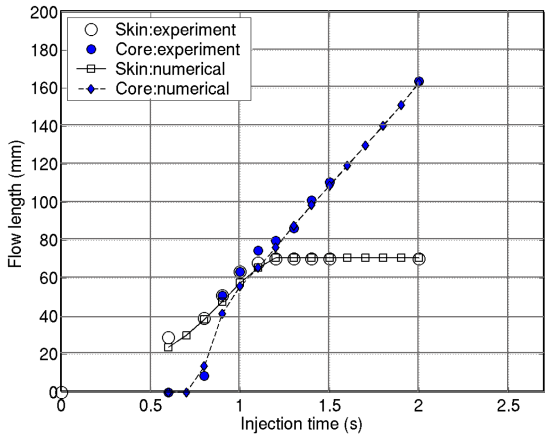

(b) Skin viscosity = middle

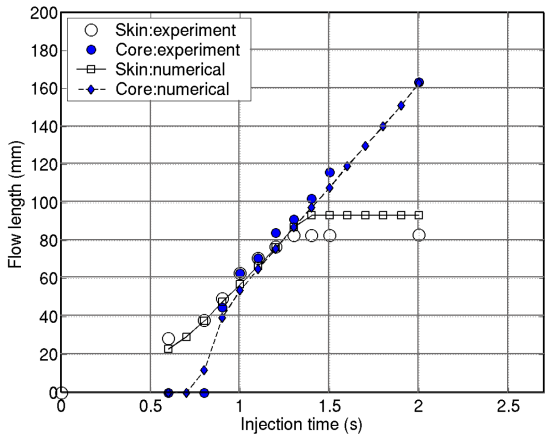

(c) Skin viscosity = low

FIGURE 6. Flow length of skin/core material for various viscosities of skin material.

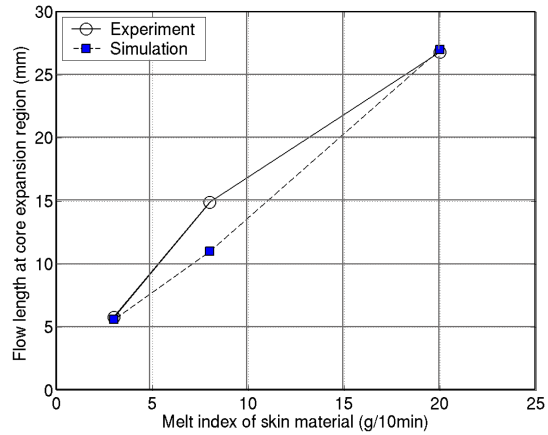

FIGURE 7. Flow length at core expansion region as function of the viscosity of skin material.

REFERENCES

1. L.S. Turng, V.W. Wang, K.K. Wang, *Trans. ASME – J. Engng. Mat. Technology,* **115**, 48-53 (1993).
2. S.C. Chen, K.F. Hsu, *Num. Heat Transfer, Part A,* **28**, 503-513 (1995).
3. F. Ilinca and J.-F. Hétu, *PPS-17, 17th Annual Conference of the Polymer Processing Society,* 12p., (2001).
4. F. Ilinca and J.-F. Hétu, *Polymer Eng. Sc.,* **43**, 1415-1427 (2003).
5. F. Ilinca and J.-F. Hétu, *Int. Polym. Proc.,* **17**(3), 265-270 (2002).
6. F. Ilinca, A. Derdouri, J.-F. Hétu, D.A. Messaoud and B. Sanchagrin, *ANTEC 2003,* 627-631 (2003).
7. F. Ilinca, J.-F. Hétu and A. Derdouri, *PPS-18, 18th Annual Conference of the Polymer Processing Society,* 19p., (2002).
8. F. Ilinca and J.-F. Hétu, *Int. J. Num. Methods Fluids,* **34**, 729-750 (2000).
9. D. Watanabe, U.S. Ishiaku, T. Nagaoka, K. Tomari and H. Hamada, *Int. Polym. Proc.*, **18**(2), 199-203 (2003).
10. D. Watanabe, U.S. Ishiaku, T. Nagaoka, K. Tomari and H. Hamada, *Int. Polym. Proc.*, **18**(4), 405-411 (2003).
11. F. Ilinca and J.-F. Hétu, *Int. Polym. Proc.,* **21**(4), 386-392 (2006).
12. F. Ilinca, J.-F. Hétu and A. Derdouri, *Int. J. Num. Methods Fluids,* **50**, 1445-1460 (2006).